

Ultrastructural Analysis of Zebra Fish (*Danio rerio*) DHDDS Retinitis Pigmentosa Disease Model Functionally Links DHDDS to Mitochondrial and Membrane Dysfunction

Jeffrey S. Prince¹, Julia Dallman², Scott Miyazaki,³ & Rong Wen⁴

Abstract

A mutation in the enzyme dehydrololichyldiphosphate synthase (DHDDS) has been causally linked to human retinitis pigmentosa (RP), a disease associated with late onset blindness due to loss of photoreceptors in the eye. Indeed, knock-down models of DHDDS in zebrafish are blind with reduced or absent photoreceptor outer segments, confirming the causal relationship between DHDDS and vision. To address mechanisms by which DHDDS knock-down disrupts photoreceptor outer segments, we used electron microscopy to examine the ultra structure of the retina at two developmental stages, one before (31 hours post-fertilization, hpf) and the other after (104 hpf) outer segments and associated vision normally develop. We identify at least three different ultra structural traits that distinguished mitochondria in DHDDS knock-down and control fish at both time points suggesting that early mitochondrial dysfunction may underlie the later deficits in the development of photoreceptor outer segments. In addition, other membrane systems (those surrounding guanine crystals in the iridophore layer and melanin pigment granules in the pigmented epithelial layer) were compromised.

Keywords: DHDDS, retina, photoreceptors, mitochondria, TEM, zebra fish, 31 and 104 hPF,

¹Department of Biology, University of Miami, Coral Gables, FL 33124 USA; & The Dauer Electron Microscopy Laboratory, Department of Biology.

²Department of Biology, University of Miami, Coral Gables, FL 33124 USA.

³Department of Biology, University of Miami, Coral Gables, FL 33124 USA.

⁴Bascom Palmer Eye Institute, University of Miami Miller School of Medicine, Miami, FL 33136, USA.

1. Introduction

Retinitis pigmentosa (RP) causes photoreceptor dysfunction and death and is characterized initially by impaired peripheral vision and eventually includes damage to central vision (Zuchner et al. 2011). Mutations in several genes (> 50) have been found to cause RP but account for only 50% of the cases (Zuchner et al. 2011). A recent study of a family of Ashkenazi Jews in which three of the four siblings had RP found a mutation in the highly conserved enzyme, DHDDS, for dolicol synthesis that appeared responsible for RP in this family when homozygous. The mutation compromises the ability of DHDDS to accomplish two enzymatic steps (the attachment of FPP, farnesyl pyrophosphate phosphate, and then 17 to 21 isoprenoid (17 to 21) units to dehydrodolichol-PP) which enables dolichol (dolicol-P) n-glycosylation of various proteins.

One of the primary components in the eye that is n-glycosylated is the pigment rhodopsin (Rho), found in the outer segment (OS, a highly modified cilium) of the photoreceptor. Injection of a splice-junction blocking morpholino (MO) against DHDDS into one cell embryos of zebrafish (*Danio rerio*) showed four day old fish (104 hpf) with behavioral responses and structural differences (the near absence of photoreceptor OS) suggestive of RP (Zuchner et al. 2011). Additional abnormalities involved other tissues.

We studied the ultrastructure of the eyes of zebra fish treated with the DHDDS knock-down versus fish without this treatment at 31 hours and 104 hrs post fertilization (= hpf), the morpholino being injected into one cell embryos. We found several changes in treated individuals that expanded the suite of alterations noted by light microscopic observation of fish treated similarly (see above, Zuchner et al. 2011): a decrease in MO treated fish of the average size of mitochondria and average total area of mitochondria in the inner segments (IS) of photoreceptors.

Additional ultrastructural characteristics that distinguished MO fish from non-treated fish included the density and extent of the retinal pigmented epithelium (RPE) in the two fish types; the size and extent of the iridophore layer encircling the latter; and the thickness of the inner plexiform layer (IPL).None of these changes have been reported before for morpholino treated zebrafish or humans with apparent RP.

2. Material and Methods

2.1. Zebrafish Preparation

The injection of the MO into one cell embryos of zebrafish was done according to Zucher et al. (2011).Fish were prepared for electron microscopy at 31 hrs and 104 hrs post fertilization (hpf).The behavioral responses of MO fish at 104 hpf were the same as those reported by Zucker et al. (2011); failing to react to light on-off switches verses that of the controls.

2.2. Transmission Electron Microscopy

Electron microscopy involved fixation in a 2.5% glutaraldehyde solution in phosphate buffer, post fixation in 1% osmium tetroxide, dehydration in a graded alcohol series, enbloch staining with uranyl acetate in 50% ethanol, and flat embeddin in L R White resin.Semi thin (1 μ m) and ultrathin(<60nm) sections were made with a Leica EMUC6 microtome and sections were viewed at 80kV with a Jeol 1400 transmission electron microscope (TEM).Image measurements utilized Imaje J 1.40 for Macintosh while semi thin section measurements used a light microscope (LM) and ocular micrometer.

Measurements of photoreceptor characteristics (TEM) were taken from photoreceptors located directly behind the lense center (Fig. 1E), measurement of the inner and outer neural plexi form layers with the LM also were located directly behind the lense.

2.3. Analysis of micrographs and statistics

The organelles in the IS of photoreceptors become polarized; 104hpf fish characteristically have a large nucleus, followed by endoplasmic reticulum, then a golgi body with several mitochondria tightly packed and adjacent to the beginning of the outer segment (OS) of the photoreceptor (Murray et al. 2009). Mitochondrial characteristics (mean area and mean total area of mitochondria per photoreceptor) were determined for only those mitochondria located above the nucleus and below the proximal terminus of the OS in both 31 and 104 hpf fish fish.

A mixed-effects model (Verbek & Molenberghs, 2009) was used to test for differences in mean mitochondrial area (MA) and total mean mitochondrial area (TA) measurements for the control versus treated group and for both the 31hpf and 104hpf fish. The interaction of the intervention with time was also tested.

3. Results

3.1. Rod ultra structure at 31 and 104 hpf

Electron microscopy showed a substantial pigmented epithelium (RPE) and large, round mitochondria above the nucleus of nascent IS rod cells in control (Ctr) fish at 31 hpf (Fig. 1 A, B). For MO fish, the RPE was essentially absent and the mitochondria had unusual shapes ranging from "Y" to oval with portions enclosing a segment of cytoplasm (Fig. 1 C, D, E).

In addition, the mitochondrial stroma of MO fish was filled with electron dense material that enhanced its contrast with the less dense intracristal spaces (Fig. 1 C, D); this was absent in Ctr fish (Fig. 1B).

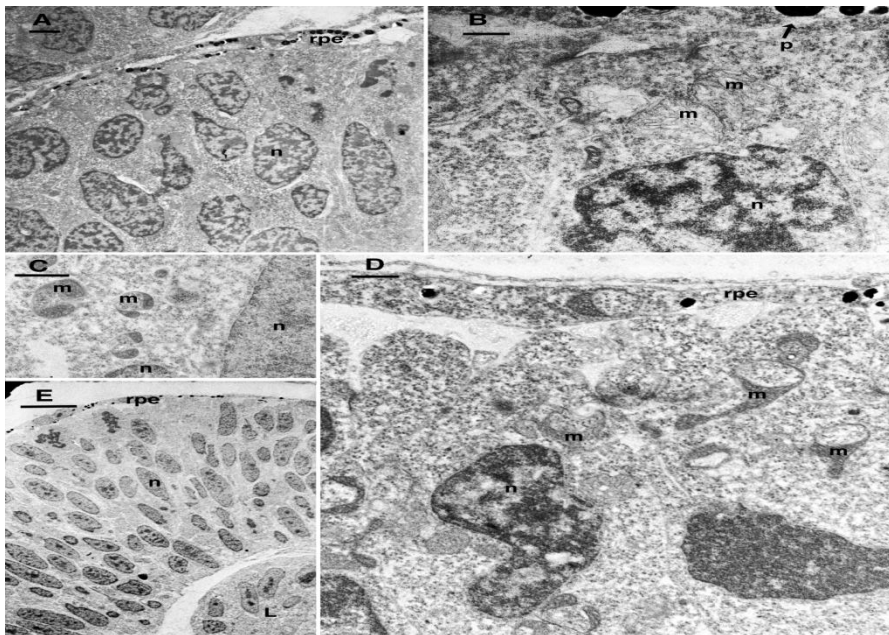


Figure 1: Ultra structure of the retina of 31hpf. Ctr(A, B) and MO fish (C, D, E)The RPE is established and mitochondria crowded at the apex of the IS (A, B).In MO fish the RPE is poorly developed (D,E) mitochondria are electron dense, have unusual shapes and not crowded against the apex of the cell (C,D).

Abbreviations: m, mitochondrion; n, nucleus; os, outer segment; p, pigment granule in the rpe; rpe, pigmented epithelium; L, lense Scale Bars: A= 5um; B= 0.5um; C= 10um;D= 2um; E= 1um.Ctr fish at 104 hpf had robust OS and RPE and the latter was surrounded by an iridophore layer (Fig. 2A, B).Mitochondria were crowded against the OS eliminating any free cytoplasmic space between them (Fig.2 B).

In 104 hpf MO fish, on the other hand, OSs were generally absent or just forming, the RPE was present but wasn't as robust as that in untreated fish (Fig. 2 C vs. A) and the iridophore layer was barely discernable (Fig. 2C). Mitochondria located at the cell apex of the IS again tended to have shapes ranging from Y to dumbbell shape, and considerable cytoplasmic space occurred between them (Fig. 2D). These mitochondria in the IS appeared more dense than those in the control for the same reasons as mentioned above for mitochondria from 31 hpf MO fish (Fig. 2 D vs. Fig. 2B).

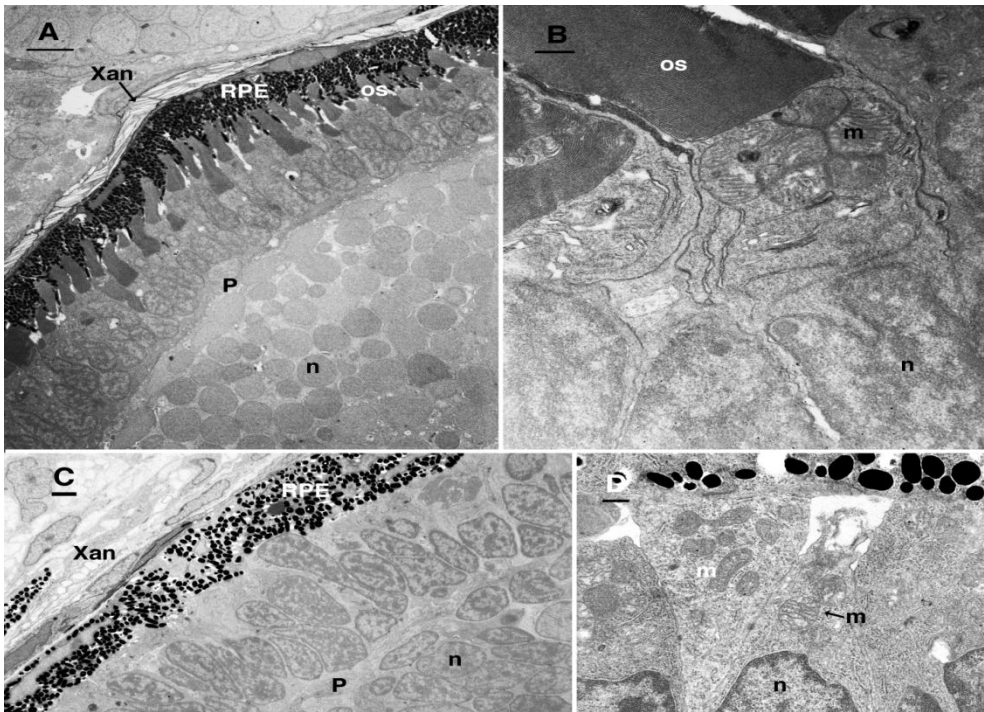


Figure 2: Ultra structure of the retina of 104hpf. Ctr (A, B) and MO fish (C, D).The iridopore layer and pigmented epithelium are apparent in the Ctr vs. MO fish (A, C).Large mitochondria are crowded above the nucleus in inner segments in the Ctr fish (B) while electron dense mitochondria have irregular shapes and dispersed above the inner segment nucleus of MO fish (D).

Abbreviations: ir, iridophore layer; m, mitochondrion; n, nucleus; os, outer segment; p, outer plexiform layer; RPE, pigmented epithelium. Scale **Bars**: A= 5 μ m; B, =0.5 μ m; C =2 μ m; D= 1 μ m

3.2. Stastical analysis The mean area (MA) and total mean area (TA) of mitochondria was significantly smaller ($p < 0.05$) in the IS of photoreceptors in MO fish verses that in Ctr fish at both 31 hpf and 104 hpf (Fig. 3 A, B and Table 1). There was no time difference for either MA or TA within either Ctr or experimental groups. After collapsing over time, there were still significant differences between Ctr and treated groups for both MA ($p < .0001$) and TA ($p = .0008$, Table 2)

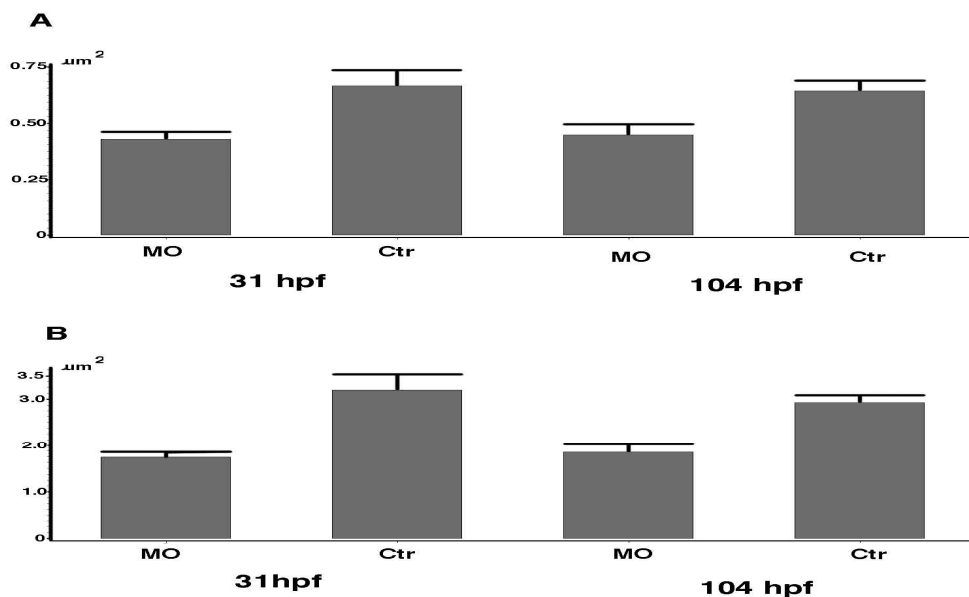


Figure 3: Mitochondrial area at two time intervals for Ctr and Mo fish. Average mitochondrion area per inner segment (A) and total mean area of mitochondria per inner segment (B). Mean \pm SEM

Table 1: Mean (MA) and total mean (TA) mitochondrial area in inner segments of photoreceptors in control (Ctr) fish and those injected with the morpholino (MO) at 31 and 104 hpf

Group	post fertiliz.	N	Mean	SD	p
Mean Mitochondrial Area					
Ctr.	31 hrs	15	0.67	0.27	0.012
MO	31	17	0.43	0.14	
Ctr.	104 hrs	20	0.64	0.21	0.024
MO	104	20	0.45	0.22	
Total Mitochondrial Area					
Ctr.	31 hrs	15	3.20	1.29	<0.0001
MO	31	17	1.74	0.47	
Ctr.	104 hrs	20	2.92	0.72	0.0008
MO	104	20	1.85	0.79	

Table 2: Mean (MA) and total mean (TA) mitochondrial area in inner segments of photoreceptors in control fish (Ctr) and those injected with the morpholino (MO) collapsing over time, 31 hpf and 104 hpf

Group	N	Mean	SD	p
31 hpf TA				
MA-Ctr.	35	0.65	0.23	p< 0.0001
MA-MO	37	0.44	0.18	
104 hpf MA				
TA-Ctr.	35	3.04	1.0	p< 0.0001
TA-MO	37	1.80	0.65	

In addition, we found a significant difference in the thickness of the outer plexiform layer (OPL) between the retinas of control and MO-treated fish with the thickness of the control fish nearly twice that in MO-treated fish (Fig. 4); no significant difference was found in the thickness of the inner plexiform layer (IPL) between the two groups (Fig. 4).

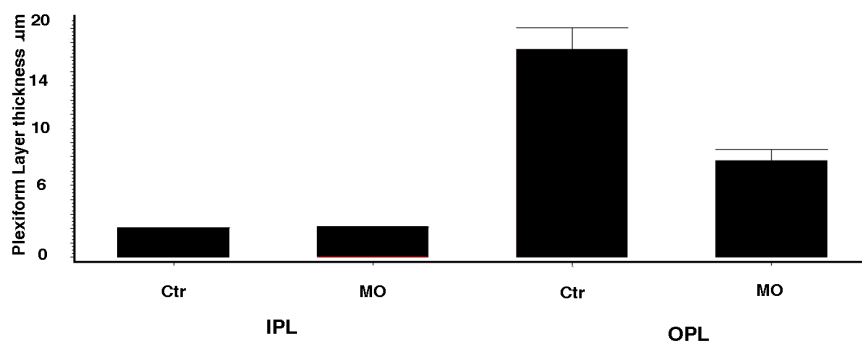


Fig 4: Thickness of the inner (IPL) and outer (OPL) plexiform layers at 104 hpf in Ctr and Mo fish. Mean \pm SEM

4. Discussion

Dolicol n-glycosylation of the visual pigment, rhodopsin, is contradicted by a knock-down mutant (MO) that compromises DHDDS' ability to activate it. Rho accounts for up to 90% of OS membrane protein (Li et al. 1994). 104hpf MO fish lack OS photoreceptors and are behaviorally blind (Zucker et al. 2011). N-glycosylation of Rho influences at least five roles that affect the proper function of the OS. These range from proper trafficking of Rho to the shedding of the OS and phagocytosis of this debris (Murray et al. 2009).

Rhodopsin is glycosylated in two regions. The second (ASN 15) is particularly important for translocation and insertion of Rho into the membrane lamella of the OS and signal transduction (Kaushal et al. 1994; Murray et al. 2009). We and Zucker et al. (2011) have both shown a lack of OS for photoreceptors in 104 hpf MO fish versus abundant OS in Ctr fish. Our findings support the importance of glycosylation of Rho for OS formation and function.

We, however, recorded additional differences between MO and Ctr fish when examined ultra structurally. The OS of photoreceptors, indeed, were lacking or insignificant in size in 104 hpf old MO fish but the mitochondria (located above the IS nucleus) were also significantly smaller in mean area and total mean area compared to Ctr fish. A similar relationship was found for Mo and Ctr fish at 31 hpf. There was no time difference effect for either Ctr or Mo groups.

Mitochondrial packing, shape, and density also varied between MO and Ctr fish. In MO fish considerable free cytoplasmic space occurred between adjacent mitochondria while Ctr fish mitochondria were tightly packed together. Mitochondria in Ctr fish at both time intervals were barrel shaped while those in MO fish ranged from "Y" to dumb bell shape and often included a cytoplasmic finger or projection. Mitochondria in MO fish had an electron dense stroma that contrasted with the less dense intracristal spaces at both time intervals; the mitochondrial stroma in Ctr IS had approximately the same density as the intracristal space (Figs 1D, E & 2 D vs. Figs 1 B & 2 B). These ultra structural changes recorded for mitochondria from MO and Ctr fish in the IS (size, shape, packing and density) probably reflects the importance of glycosylation of mitochondrial proteins for the proper function of this organelle (Briones et al. 2001; Burnham-Marusch & Berninsone, 2012; Gao et al. 2002; Gawlowski et al. 2012).

The morphological changes in mitochondria appeared within the first few hours after injection of the morpholino while other morphological traits such as OS size or presence took longer to appear. Furthermore, the difference in mean area and total mean area did not change significantly between 31 hpf and 104 hpf in either MO or Ctr fish. This might be explained by rapid mitochondrial development in control fish in order to provide energy for OS development and maintenance versus continued mytodysfunction in MO fish.

We also noted additional changes in the abundance of pigment granules (melanosomes; Szamier and Berson, 1977), making up the RPE, and the size and extent of the reflective iridophore layer (of pure guanine in hydrated crystalline form; Rohrlig & Rubin, 1975) that surrounds the RPE in fish. MO treated fish at both time intervals had a reduced RPE. The melanin pigment is surrounded by a membrane that also requires glycosylation (Szamier and Berson, 1977). The iridophore layer is absent at 31 hpf in both MO and Ctr fish but present in 104 hpf Ctr fish but virtually absent in the 104 hpf MO fish. The guanine crystals are also membrane bound (Rohrlig, 1974) and like many secreted membranes and nucleocystolic proteins probably require glycosylation for proper membrane formation and function (Burnham-Marusich & Berninsone, 2012); this is inhibited in MO fish.

Finally, the inner plexiform layer was considerably thinner in MO vs Ctr fish at 104 hpf; no difference was seen for the OPL layer for the same fish. Animal models of RP have found rhodopsin positive neurites sprouting from surviving rods but do not mention additional effects on either the IPL or OPL. Tunicamycin inhibition of neurite outgrowth closely matches that of Mo knock-down effect on dolicol n-glycosylation (Heacock, 1982). The lack of neurite development in MO fish in the IPL again might be due to the negative effect of the lack of glycosylation on cell membranes (Burnham-Marusich & Berninsone, 2012).

Acknowledgements

We would like to thank Dr. William LeBlanc (thedata doctor@gmail.com) for assistance with statistical analyses and financial assistance from the Dauer Electron Microscopy Laboratory, Biology Department, and University of Miami.

References

- Briones, P. Vilaseca, M.A. Garcia-Silva, M.T. Pineda, M. Colomer, J. Ferrer, I. Artigas, J. Jaeken, A and A. Chabas. (2001). Congenital disorders of glycosylation (CDG) may be underdiagnosed when mimicking mitochondrial disease. *European Journal of Paediatric Neurology* 5:127-131.
- Burnham-Marusich, A.R and P.M. Berninsone. (2012). Multiple proteins with essential mitochondrial functions have glycosylated isoforms. *Mitochondrion* 12:423-427.
- Gao, J. Cheon, K. Nusinowitz, S. Liu, Q. Bei, D. Atkins, K. Azimi, A. Daiger, S.P. Faber, D.B. Heckenlively, J.R. Pierce, E.A. Sullivan, L.S. and J. Zuo. (2002). Progressive photoreceptor degeneration, outer segment dysplasia, and rhodopsin mislocation in mice with targeted disruption of the retinispigmentosa-1 (Rp-1) gene. *Proc. Natl. Acad. Sci.* 99:5698-5703.
- Gawlowski, T. Suarez, J. Scott, B. Torrez-Gonzalez, M. Wang, H. Schwappacher, R. Han, X. Yates III, J.R. Hoshijima, M. and W. Dillman. (2012). Modulation of dynamin-related protein 1 (DRP1) function by increased *O*-linked-N-acetylglucosamine modification (*O*-GlcNAc) in cardiac myocytes. *Journal of Biological Chemistry*. 287:30024-30034.
- Heacock, A.M. (1982). Glycoprotein requirement for neurite outgrowth in goldfish retina explants: Effects of tunicamycin. *Brain Research* 241:307-315.
- Kaushal, S. Ridge, K.D. and H.G. Khorana. (1994). Structure and function in rhodopsin: The role of asparagine-linked glycosylation. *Proc. Natl. Acad. Sci.* 91:4024-4028.
- Li, Z-Y, Jacobson, S.G. and A.H. Milam. (1994). Autosomal dominant retinitis pigmentosa caused by the threonine-17-methionine mutation: Retinal histopathology and immunochemistry. *Exp. Eye Res.* 58: 397-408.
- Murray, A.R., Fliesler, S. J. and M.R. Al-Ubaidi. (2009). Rhodopsin: The functional significance of Asn-linked glycosylation and other post-translational modifications. *Ophthalmic Genetics* 30:109-120.
- Rohrlig, S.T. (1974). Fine structural demonstration of ordered arrays of cytoplasmic filaments in vertebrate iridophores. *Journal of Cell Biology*. 62: 295-304.

- Rohrlic, S.T. and R.W. RTubin. (1975). Biochemical characterization of crystals from the dermal iridophores of Chameleon *Anolis carolinensis*. *Journal of Cell Biology* 66: 635-645.
- Szamier, B.R. and E.L. Berson. (1977). Retinal ultrastructure in advanced retinitis pigmentosa. *Invest. Ophthalmol. Visual Sci.* 16:947-962.
- Züchner, S. Dallman, J. Wen, R. Beecham, G. Naj, A. Farooq, A. Kohli, M.A. Whitehead, P.L. Hulme, W. Konidari, I. Edwards, Y.J.K. Cai, G. Peter, I. Seo, D. Buxbaum, J.D. Haines, J.L. Blanton, S. Young, J. Alfonso, E. Vance, J.M. Lam, B.L., and M. A. Vance. (2011) Whole-Exome Sequencing Links a Variant in DHDSD to Retinitis Pigmentosa. *American Journal of Human Genetics* 88:201-206.
- Verbeke, G, & Molenberghs, G. (2009). *Linear Mixed Models for Longitudinal Data*. New York, NY: Springer.